TENSOR SCALE-BASED ANISOTROPIC REGION GROWING FOR SEGMENTATION OF ELONGATED BIOLOGICAL STRUCTURES

Ziyue Xu[1] *Zhiyun Gao*[1] *Eric A. Hoffman*[2] *Punam K. Saha*[1,2]

[1] Department of Electrical and Computer Engineering
[2] Department of Radiology
University of Iowa, Iowa City, IA 52242

ABSTRACT

Over decades, segmentation has remained a salient task in most medical imaging applications confronting multi-faced challenges including limited image quality. In this paper, we present a new anisotropic region growing segmentation approach for vascular or other elongated structures. A fundamental challenge during tracing vascular structures is broken continuity of structures by noise and other imaging artifacts coupled with leaking through blurring and soft boundaries. Anisotropic region growing solves this problem using tensor scale that captures local structure orientation and geometry using an ellipsoidal model. A new fuzzy connectivity based algorithm is developed that uses tensor scale to facilitate region growing along the local structure while arresting cross-structure leaking. The performance of the method has been quantitatively evaluated on non-contrast human pulmonary C-T imaging and the results found are promising.

Index Terms— image segmentation, tensor scale, fuzzy connectivity, local parameter control, anisotropic region growing

1 Introduction

Analysis of vascular geometry is important in many medical imaging research including pulmonary, cardiac and carotid applications. Several segmentation approaches, including manual outlining, boundary based [1], region-based [2], and shape and model-based [3] techniques have been introduced and subsequently modified and investigated in different applications. In this paper, we develop a new anisotropic region growing algorithm with target application to segmentation of vasculature and elongated structures. Region growing approach was adopted for this purpose because - (1) high inter-subject variations vascular shape and topology even for a specific body region, (2) high complexity of vascular geometry and topology.

The aim of this paper is to develop a local structure controlled anisotropic region growing method. Fuzzy connectivity [4, 5] has become a popular method where, the region growing is governed by a predefined fuzzy affinity relation. The fuzzy connectivity theory was proposed by Rosenfeld which was which was fundamentally remodeled and introduced in segmentation by Udupa *et al* [5]. Saha and Udupa [6] introduced the notion of scale in the fuzzy connectivity framework. A fundamental challenge with this approach in the context of tracing a vasculature in an image with limited signal-to-noise ratio emerges out of broken continuity of structures by noise and other artifacts coupled with blurring and soft boundaries. The anisotropic region growing solves this problem using tensor scale [7] that captures local structure orientation and geometry using an ellipsoidal model. A new fuzzy connectivity based anisotropic region growing algorithm has been developed that uses tensor scale to facilitate region growing along local structure while arresting cross-structure leaking. In our approach, anisotropy of local structures through tensor-scale is incorporated into the theoretical fuzzy connectivity model through a new local parameter control strategy. The notion of a tensor scale - a unified representation of local structure size, orientation and anisotropy was introduced by Saha [7]. Recently, a precise analytic definition of tensor scale and an effective computational solution in 3- or higher-dimensional images [8] have been developed. Tensor scale carries the promise of serving as a rich parametric descriptor of local geometry that may benefit several image processing applications.

2 Theory and algorithms

In this section, we first briefly present fuzzy connectivity [5] and tensor scale [7]. Subsequently, we introduce the theory and algorithm of a new anisotropic region growing algorithm that combine the above two methods to facilitate along-structure growing while constraining cross-structure leaking.

Let $\mathbb{Z}^3$ denote a three-dimensional (3D) cubic grid representing the *image space* where $\mathbb{Z}$ is the set of integers; each element of $\mathbb{Z}^3$ is called a *voxel*. An image on $\mathbb{Z}^3$ may be defined by an *image intensity function* $f : \mathbb{Z}^3 \rightarrow \mathbb{Z}^+$, where $\mathbb{Z}^+$ is the set of positive integers. A fuzzy relation $\mu_\alpha : \mathbb{Z}^3 \times \mathbb{Z}^3 \rightarrow \{0, 1\}$ referred to as *adjacency* is used to determine closeness of two voxels in the image space. A path π is a sequence $\langle p_1, p_2, ..., p_l \rangle$ where every two successive voxels are adjacent. Path strength $\mu_{\mathcal{N}}(\pi)$ is defined as:

$$\mu_{\mathcal{N}}(\pi) = \min_{1 \leq i < l} \mu_\kappa(p_i, p_{i+1}).$$

where $\mu_K(p,q)$, referred to as fuzzy affinity, captures the local hanging-togetherness between p and q, i.e., the strength of the link $\langle p,q\rangle$. Fuzzy connectedness between two voxels p,q is the strength of the strongest path between them, i.e.,

$$\mu_K(p,q) = \max_{\pi\in\mathcal{P}(p,q)} \mu_{\mathcal{N}}(\pi).$$

where, $\mathcal{P}(p,q)$ denotes the set of all paths between p,q.
A fuzzy connected objet $\mathcal{O}$ in an image is defined as the region grown from a predetermined set of seeds, say S. Thus, the membership-function of $\mathcal{O}$ may be defined as follows:

$$\mu_{\mathcal{O}}(p) = \max_{s\in S} \mu_K(p,s).$$

It has been shown in [9], that fuzzy connectivity is a similitude fuzzy relation and an efficient computational solution was presented in [5].
Tensor scale is defined on an image $\mathbb{I}$ in 3D continuous space $\mathbb{R}^3$, where $\mathbb{R}$ denote the set of real numbers. $\mathbb{I}$ is considered as the union of multiple objects which are defined as partitions by M 2D pseudo-Riemannian manifolds, say, $m_1, m_2, ..., m_M$; we refer to these manifolds as *partitioning manifold*. Now, let us first consider a point $p \in \mathbb{R}^3$ and the subspace W_i formed by a set of i orthogonal vectors $\boldsymbol{\tau}_1(p), \boldsymbol{\tau}_2(p), ..., \boldsymbol{\tau}_i(p)$ with p being the origin. An image with partitioning manifolds $W_i^{\perp} \cap m_1, W_i^{\perp} \cap m_2, ..., W_i^{\perp} \cap m_M$ is formed over the orthogonal complement $W_i^{\perp}$ of W_i. Let us refer to this image as as orthogonal complement image of the vectors $\boldsymbol{\tau}_1(p), \boldsymbol{\tau}_2(p), ..., \boldsymbol{\tau}_i(p)$ at p. Finally, tensor scale at a point $p \in \mathbb{R}^3$ is an ordered sequence of 3 orthogonal vectors $\langle \boldsymbol{\tau}_1(p), \boldsymbol{\tau}_2(p), \boldsymbol{\tau}_3(p)\rangle$ inductively defined as follows:
1. $\boldsymbol{\tau}_1(p)$ is the vector from p to the closest point on a partitioning manifold of $\mathbb{I}$.
2. Given the first i orthogonal vectors, $\boldsymbol{\tau}_1(p), \boldsymbol{\tau}_2(p), ..., \boldsymbol{\tau}_i(p)$, the $(i+1)$th vector $\boldsymbol{\tau}_{i+1}(p)$ points from p to the closest point on a partitioning manifold in the orthogonal complement image of $\mathbb{I}$ induced by $\boldsymbol{\tau}_1(p), \boldsymbol{\tau}_2(p), ..., \boldsymbol{\tau}_i(p)$ at p.
$\boldsymbol{\tau}_1(p)$, $\boldsymbol{\tau}_2(p)$ and $\boldsymbol{\tau}_3(p)$ will be referred to as primary, secondary and tertiary tensor vectors of p. The notion of tensor scale defined as above is schematically illustrated in Fig. 1 with a 3D rabbit femur bone surface m_1. The primary vector $\boldsymbol{\tau}_1(p)$ (red) defines the direction and distance to the closest point on the femur surface. The orthogonal complement plane $W_1^{\perp}$ and the 1D partitioning manifold $W_1^{\perp} \cap m_1$ on $W_1^{\perp}$ are shown in the figure; note that the 1D partitioning manifold (cyan) is essentially the intersection between the plane $W_1^{\perp}$ (blue) and the partitioning surface m_1 (the femur bone surface) in the 3D image. The secondary t-vector $\boldsymbol{\tau}_2(p)$ (yellow) is defined by the point on $W_1^{\perp} \cap m_1$ that is closest to p. Once $\boldsymbol{\tau}_1(p)$ and $\boldsymbol{\tau}_2(p)$ are found, the line (dotted green) on which the tertiary t-vector $\boldsymbol{\tau}_3(p)$ (green) lie is confirmed; the final direction and the length of $\boldsymbol{\tau}_3(p)$ is defined by finding the closest point on the partitioning surface along the line.

2.1 Tensor scale based anisotropic region growing

Effectiveness of fuzzy connectivity is highly dependent on the choice of the affinity relation. A major challenge with fuzzy connectivity analysis of pulmonary vasculature is that vessels form a tree-like structure of tubular paths and at fine scales, the diameter of these paths may be comparable to voxel resolution. Therefore, these tubular paths, especially at finer scales, are vulnerable and may get broken by noise or other imaging artifacts and the continuity of vascular structure may be lost using a region growing rules suitable for other regions. On the other hand, softening the rules to capture the broken continuity may cause leaking through other regions. However, a human expert may capture the broken continuity implicitly using the contextual knowledge of local structures. Here, we develop an anisotropic region growing algorithm where the growing rules adapt to local structure geometry. To solve this problem, we use tensor scale that gives an ellipsoidal representation of the local structure at every image point and construct a local structure-adaptive formulation of the fuzzy affinity function as described in the following.

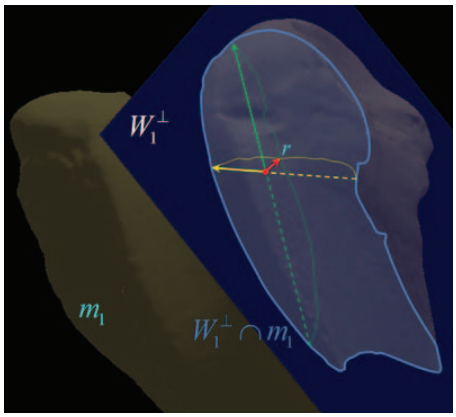


Fig. 1: An illustration of tensor scale using a rabbit femur bone surface (dark off-white) forming a 2D manifold m_1. The candidate spel p is shown as a red dot; see text for detail.

Saha and Udupa [6] presented a thorough discussion on fuzzy affinity using local scale. However, local structure anisotropy to control affinity function in a direction-dependent fashion was not addressed. As recommended in [7], the following formulation of affinity function is used:

$$\mu_\kappa(p,q) = \begin{cases} 1, & \text{if } p = q; \\ \mu_\alpha(p,q)\sqrt{\mu_\psi(p,q)\mu_\phi(p,q)}, & \text{otherwise.} \end{cases}$$

where μ_α, μ_ψ and μ_ϕ are adjacency, homogeneity and object feature based components of "local hanging-togetherness" in the fuzzy affinity function.
Here, we present tensor scale based formulation of these functions. The adjacency function μ_α is defined using tensor scale as follows $\mu_\alpha(p,q) = 1$, if p and q fall inside each other's tensor scale ellipsoid and '0' otherwise. $\mu_\psi(p,q)$ captures homogeneity between p and q and $\mu_\phi(p,q)$ gives the hanging-togetherness of p and q in the target object based on likeliness of their feature values with respect to the expected feature distribution of the target object. It was argued in [7] that the function μ_ψ should be chosen to reflect the measure

of the fuzzy proposition "x is small" while the other function μ_ϕ should be chosen to reflect the measure of the fuzzy proposition "x is close to an expected value". The following functional forms are used here.

$$\mu_\psi(p,q) = e^{-\frac{|f(p)-f(q)|^2}{2\sigma_\psi^2}}, \text{and}$$

$$\mu_\phi(p,q) = \min\left(e^{-\frac{|f(p)-m|^2}{2\sigma_\phi^2}}, e^{-\frac{|f(q)-m|^2}{2\sigma_\phi^2}}\right),$$

where σ_ψ and σ_ϕ are two different standard deviation parameters used for homogeneity and object feature distribution and m is the mean object feature value. When these parameters are large, the object grows more generously and possibilities of leaking through boundaries increase. On the other hand, when small values are used for these parameters, the growth process works conservatively and the chance of breaking object continuity due to noise and other imaging artifacts increases. In the conventional region growing methods [10, 11], these parameters was kept fixed and fine control on and adaptivity to local structural properties was lacking. The key idea and contribution of our anisotropic region growing is to locally adapt these two parameters σ_ψ and σ_ϕ in an orientation-adaptive manner using local tensor scale to enhance compliance of region growing with the context of local structures. Specifically, the two controlling parameter σ_ψ and σ_ϕ are determined by local tensor scale in a space- and orientation-variant manner as follows:

$$\sigma_X(p,q) = \sigma_{X,\text{stationary}} + \chi\left(\max\left(\zeta_p(q), \zeta_q(p)\right)\right)\sigma_{X,\text{adaptive}},$$

where $X \in \{\psi, \phi\}$, $\zeta_p(q)$ is the size of tensor scale ellipsoid at p along pq. χ is a monotonically non-decreasing function, e.g.,

$$\chi(x) = \begin{cases} 1, & \text{if } x > x_{\max}; \\ \frac{1+x}{1+x_{\max}}, & \text{otherwise.} \end{cases}$$

The value of $x_{\max}$ is determined as the rough estimate of the maximum scale of the target object. The two parameters $\sigma_{X,\text{stationary}}$ and $\sigma_{X,\text{adaptive}}$ are the stationary and adaptive components in the control parameter; here, we have used one third of the total control parameter remain stationary while the two-third fraction is varied by local tensor scale; thus, the ratio of $\sigma_{X,\text{stationary}}$ and $\sigma_{X,\text{adaptive}}$ $1:2$. Finally, the total value of the control parameter, i.e., $\sigma_{X,\text{stationary}} + \sigma_{X,\text{adaptive}}$ is determined following the description in [12].

3 Results

Results of several qualitative and quantitative evaluative experiments are presented. Fig. 2 presents the results of application of the new method and its comparison with the conventional fuzzy connectivity region growing [5] on a 2D photographic image of a coral reef containing a complex tree-like network of locally elongated fuzzy branch structures. As shown Fig. 2(a), one seed (red-cross) was manually selected on the main trunk of the coral reef tree and the results of application using the conventional and the anisotropic region growing methods are shown in Fig. 2(b,c), respectively. As observed in Fig. 2(b,c), the new method (Fig. 2(c)) captures more branch structures, especially at low-contrast regions where the vessel got broken by imaging artifacts and noise and it is more prominent in the zoomed in displays of Fig. 2(d-f).

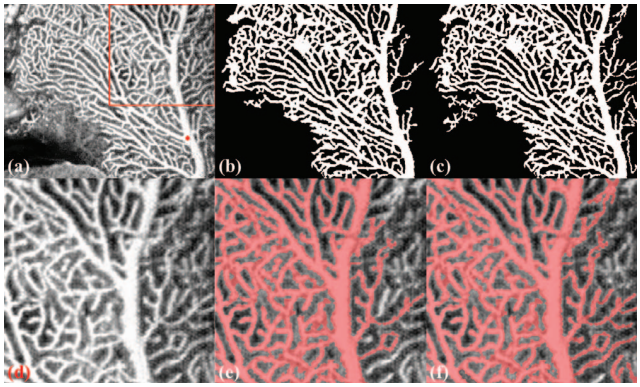


Fig. 2: 2D Segmentation results on an image of coral reef (a); the red-cross indicates the seed. The new anisotropic region growing has captured more branches (c) as compared to the conventional algorithm (b). (d-f) Zoomed-in display of (a-c) over the regions marked by the red box in (a).

Two non-contrast pulmonary human CT images acquired with voxel size of $0.55 \times 0.55 \times 0.5mm^3$ and in-plane matrix of 512×512 was used to quantitatively evaluate the new method's performance in comparison with Shikata's method [13]. One seed point in the cardiac region was manually selected for applying the new anisotropic diffusion algorithm for vascular segmentation. Initial results of anisotropic region growing are shown in Fig. 3(b). The new method has successfully captured structures at a wide range of scales including those at high and small scales. Pulmonary vessel was separated from cardiac and other tissue regions by putting a separator on pulmonary trunk and separating the pulmonary vasculature from the rest of the tissue using the multi-scale opening algorithm [14]. Result of pulmonary vasculature after removing the heart and other body regions is shown in Fig. 3(c) and (e). Results of vascular segmentation using Sikata's method are shown in Fig. 3(d) and (f).

Although, the method by Shikata was able to capture medium scale vessels, its performance was somewhat compromised at fine and large scale. 3D rendition of vasculature using our method and Shikata's method are presented in Fig. 3(e,f), respectively. 3D rendition confirmed our observations in 2D. Vessel segmentation results using anisotropic region growing algorithm capture more details at large and small scales and also maintain better vascular topology around the pulmonary entry region as compared to Shikata's method due to the compromised behavior of the later method at large scales.

To quantitatively evaluate the performance of the two methods, we used manually selected points inside and outside vascular regions those were used as ground truth for accuracy

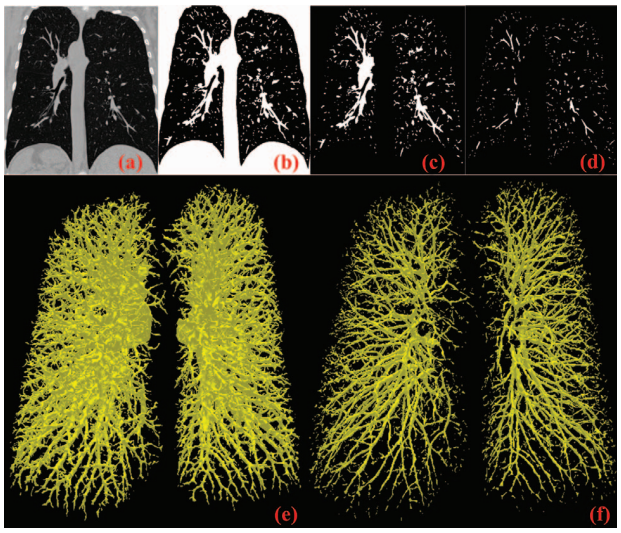


Fig. 3*:* Results of vascular segmentation in non-contrast human pulmonary CT imaging. (a) A 2D CT image slice. (b-c) Vessel segmentation on the matching slice using the anisotropic region growing (b: before peripheral tissue removal; c: final vessel segmentation) and the Shikata's (d) algorithms. (e,f) 3D renditions of vasculature using the new (e) and Shikata's (f) methods.

and error evaluation. Specifically, 1000 points were manually selected by an expert inside the vascular region on randomly picked slices; another set of 1000 points were selected outside the vascular region. Visually confirmed vessels over the entire range of scales were used to select these points; finally, the points outside the vessels were selected no further than 3 voxels from the vessel region as determined visually. Let V denote the set of points manually selected on vascular region and let B denotes the set of points manually selected outside the vascular region. Let V_C and B_C denote the set of points on vascular region on its complement derived using a given algorithm. $Accuracy = \frac{|V \cap V_C| + |B \cap B_C|}{|V| + |B|}$, $Error = \frac{|V \cap B_C| + |B \cap V_C|}{|V| + |B|}$

Table 1*:* Results of accuracy analysis of vessel segmentation by the two methods.

	Data set 1		Data set 2	
	T-scale	Shikata	T-scale	Shikata
Accuracy	97.6%	91.5%	96.9%	79.0%
Error	2.4%	8.5%	3.1%	21.0%

T-scale computation is a computationally involved task and it takes approximately 60 minutes for a $512 \times 512 \times 676$ image. Once it is computed, the anisotropic region growing is relatively fast and takes only 2-3 minutes for such images. Performance measures for the two methods on two different datasets are presented in Table 1. The new method has produced high accuracy for both datasets while the Shikata's method produced significantly lower accuracy for the second dataset which was caused by missing an entire vascular branch due to its compromised performance at large scales.

4 Conclusion

A new fuzzy connectedness based anisotropic region growing algorithm has been developed that combines tensor scale with fuzzy connectivity facilitating region growth along local structures while arresting cross-structure leaking. By incorporating tensor scale information, the algorithm locally adapts and governs the fuzzy segmentation process so that it can capture vascular structures more robustly in the presence of noise and other imaging artifacts. Application of the method to pulmonary images demonstrates promising quantitative results. In our future research, we will use additional structural features to further improve the performance of the current scheme.

5 References

[1] M. Kass, A. Witkin, and D. Terzopoulos, "Snakes: Active contour models," *Int. J. of Comp. Vis.*, vol. 1, no. 4, pp. 321–331, 1988.

[2] J. K. Udupa, P. K. Saha, and R. A. Lotufo, "Relative fuzzy connectedness and object definition: Theory, algorithms, and applications in image segmentation," *IEEE Trans. Pattern Anal. Mach. Intell.*, vol. 24, pp. 1485–1500, 2002.

[3] T. F. Cootes, C. J. Taylor, D. H. Cooper, and J. Graham, "Active shape models their training and application," *Comput. Vis. Image Underst.*, vol. 61, pp. 38–59, 1995.

[4] A. Rosenfeld, "Connectivity in digital pictures," *J. ACM*, vol. 17, pp. 146–160, 1970.

[5] J. K. Udupa and S. Samarasekera, "Fuzzy connectedness and object definition: Theory, algorithms, and applications in image segmentation," *CVGIP: Graphical Model and Image Processing*, vol. 58, no. 3, pp. 246–261, 1996.

[6] P. K. Saha, J. K. Udupa, and D. Odhner, "Scale-based fuzzy connected image segmentation: theory, algorithms, and validation," *Comput. Vis. Image Underst.*, vol. 77, pp. 145–174, 2000.

[7] P. K. Saha, "Tensor scale: a local morphometric parameter with applications to computer vision and image processing," *Comput. Vis. Image Underst.*, vol. 99, pp. 384–413, 2005.

[8] P. K. Saha and Z. Xu, "An analytic approach to tensor scale with an efficient algorithm and applications to image filtering," in *Proc. Int. Conf. DICTA, 2010*, 2010, pp. 429 –434.

[9] P. K. Saha and J. K. Udupa, "Fuzzy connected object delineation: Axiomatic path strength definition and the case of multiple seeds," *Comput. Vis. Image Underst.*, vol. 83, no. 3, pp. 275 – 295, 2001.

[10] Y. L. Chang and X. Li, "Adaptive image region-growing," *IEEE Trans. Image Processing,*, vol. 3, no. 6, pp. 868 –872, 1994.

[11] S. C. Zhu and A. Yuille, "Region competition: Unifying snakes, region growing, and bayes/mdl for multi-band image segmentation," *IEEE Trans. Pattern Anal. Mach. Intell.*, vol. 18, pp. 884–900, 1996.

[12] P.K. Saha and J.K. Udupa, "Scale-based diffusive image filtering preserving boundary sharpness and fine structures," *IEEE Trans. Med. Imag.*, vol. 20, no. 11, pp. 1140 –1155, 2001.

[13] H. Shikata, E. A. Hoffman, and M. Sonka, "Automated segmentation of pulmonary vascular tree from 3D CT images," in *SPEI: Medical Imaging*, 2004, vol. 5369, pp. 107–116.

[14] P. K. Saha, Z. Gao, S. K. Alford, M. Sonka, and E. A. Hoffman, "Topomorphologic separation of fused isointensity objects via multiscale opening: Separating arteries and veins in 3-d pulmonary ct," *IEEE Trans. Med. Imag.*, vol. 29, no. 3, pp. 840 –851, 2010.